Temporal evolution of mesoscopic structure of some non-Euclidean systems using a Monte Carlo model

T. Mazumdar,[1] S. Mazumder,[2,*] and D. Sen[2]

[1]*Research Reactor Services Division, Bhabha Atomic Research Centre, Mumbai-400 085, India*

[2]*Solid State Physics Division, Bhabha Atomic Research Centre, Mumbai-400 085, India*

(Received 4 October 2010; revised manuscript received 23 January 2011; published 23 March 2011)

A Monte Carlo–based computer model is presented to explain the contrasting observations of Mazumder *et al.* [Phys. Rev. Lett. **93**, 255704 (2004) and Phys. Rev. B **72**, 224208 (2005)], based on neutron-scattering measurements, on the temporal evolution of the effective fractal dimension and the characteristic length for hydration of cement with light and heavy water. In this context, a theoretical model is also proposed to elucidate the same.

DOI: 10.1103/PhysRevB.83.104302 PACS number(s): 64.75.−g, 61.43.Hv, 61.50.Ks

I. INTRODUCTION

Dispersion of liquids in solids leading to gel formation is a diffusion-controlled process. Diffusion in Euclidean geometry is formulated theoretically by the random walk of a drunken walker in Euclidean space. Gelation of silicates, a cementitious material, leads to mesoscopic structures with non-Euclidean fractal morphology in a length scale of order $10-10^4$ Å. Diffusion in non-Euclidean fractal geometry is similar, in physical terms, to the random walk of a drunken walker on a road system designed by another drunken engineer—theoretical formations of which are not satisfactorily comprehensible[1,2] yet like dynamics of many hydration reactions. It is shocking that investigation of cement is still in its infancy despite the fact that cement is a ubiquitous material which is indispensable in the construction industry, in nuclear energy programs for immobilization of non-heat-generating low-level radioactive waste, and in the petroleum industry to line oil wells by pumping cement slurry to isolate productive zones. Global production of cement exceeds that of any other material of technological importance. The total world consumption of cement in 2008 was about 2.5 billion metric tons, almost double of that of steel. Manufacturing of cement contributes about 4% of global and 5%–7% of total man-made CO_2 emissions. The understanding of the mechanism of its hydration and evolution of cement-water mixtures into a material of high compressive strength is paramount to improve its lifetime and other macroscopic properties such as compressive strength, permeability, elastic modulus, etc.

Cement reacts with light water via a hydration reaction which yields an amorphous calcium silicate hydrate (C-S-H) gel-like structure and crystalline calcium hydroxide as the main products. To elucidate the microscopic structure of the C-S-H gel, many models[3–8] have been proposed. Investigations, based on small-angle neutron scattering (SANS), on continuous temporal evolution of mesoscopic structure during hydration of cement are recent.[9–11] SANS measurements involve mapping of the time-dependent scattering function $S(q,t)$ where t stands for time and q is the modulus of the scattering vector $\boldsymbol{q}$. Because of the isotropic nature of the system at the mesoscopic scale, $S(q,t)$ is a function only of q. For all the experimental measurements of concern, it has been observed that $S(q,t)$ asymptotically approaches a form $S(q,t) \sim q^{-\eta(t)}$. The exponent η, associated with power-law scattering, reflects[12] directly the mass fractal dimension D_m. For a mass fractal object, $\eta = D_m$ with $1 < \eta < 3$ and $1 < D_m < 3$. For objects whose surface is fractal, the exponent η is related[13] to the surface fractal dimension D_s with $3 < \eta < 4$ and $2 < D_s < 3$.

The investigations[2,9–11,14] on hydration of silicates and sulfates with light water (H_2O) and heavy water (D_2O) report some seemingly incomprehensible results. It is observed that the kinetics of hydration of silicates and sulfates are of nonlinear nature even at the initial time. In the case of hydration of silicates with light water, the hydrating mass exhibits a mass fractal nature throughout the hydration, with the mass fractal dimension increasing with time and reaching a finite saturation value at large time. The second phase grows with time initially. Subsequently, the domain size of the second phase saturates. It has also been demonstrated that light water hydration of silicates exhibits a scaling phenomenon for a characteristic length $L(t)$ with a measure of curvature of the normalized[2] time-dependent scattering function $S(q,t)$.

For a monodisperse population of spheres of radius R, $L(t) = R\sqrt{2/5}$. For a polydisperse population of spheres, with number density $\rho(R)$ of radius R, $L(t) = \sqrt{2\langle R^8\rangle/5\langle R^6\rangle}$ where $\langle R^n\rangle$ is the nth moment of the distribution $\rho(R)$. The temporal behavior of the characteristic length has been observed to be far from a power law. Further, temporal evolution of $\{L(t)\}^2$ nearly mimics the trend of evolution of D_m. D_m also reaches a plateau almost at the same time (see Fig. 1 for hydration of tricalcium silicate with a light water to cement ratio of 30%). It is interesting to note that these observations indicate that both physical quantities, the characteristic length and effective fractal dimension in the length scale (it is basically the effective fractal dimension for length scales from 10^3 to 10^4 Å; for simplicity we call it fractal dimension everywhere in the text), having different dimensionalities (as the fractal dimension is a dimensionless quantity while the characteristic length has the dimension of length), reach a plateau almost at the same time and in a similar fashion. We want to understand whether the similarity of temporal evolutions of two altogether different physical quantities is an accidental one or not. But repeated measurements,[2] varying over a wide range of compositions, brought out this phenomenal accidental similarity.

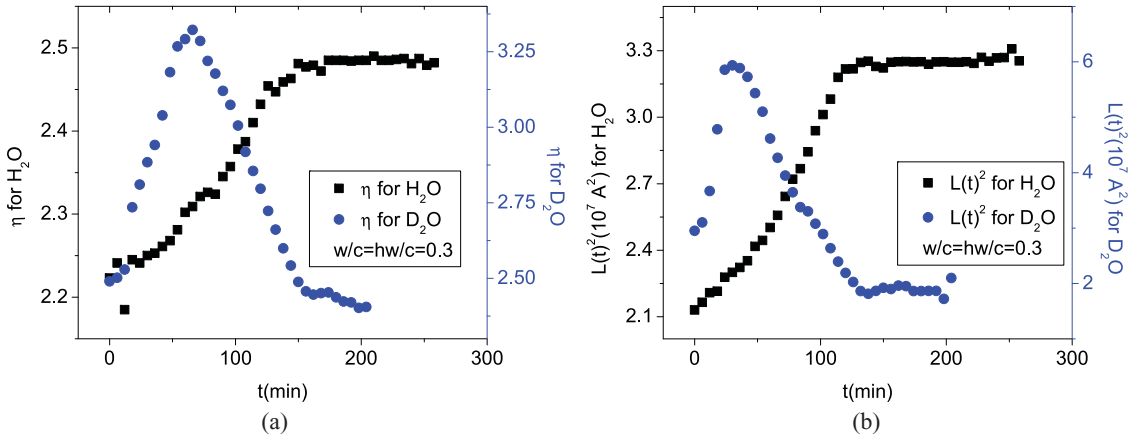

FIG. 1. (Color online) Temporal evolution of (a) η and (b) $[L(t)]^2$ for both light water and heavy water hydrating silicates as observed from neutron scattering measurements (Ref. 1). Only a typical representative figure is considered. For light water hydrating silicates, both η and $[L(t)]^2$ increase with time and reach a plateau, whereas for heavy water hydrating silicates, they first increase, then reach a peak, and finally decrease as time increases.

As far as chemistry is concerned, the hydration of silicates with light and heavy water is expected to be quite similar except for kinetics. Due to the different molecular masses of light and heavy water, diffusion is expected to be more sluggish for heavy water. Further, it is known that the hydrogen bond with deuterium is slightly stronger than the one involving ordinary hydrogen.[15] The lifetime of the hydrogen bond involving D is longer than that involving H because the libration motions perpendicular to the bond direction have smaller amplitude for D than for H, because of the difference of masses. If diffusion is the only controlling factor, the hydration of cement with H_2O and D_2O is expected to be quite similar except for kinetics, as diffusion of D_2O is somewhat sluggish because of its heavier molecular mass compared to H_2O.

However, some incomprehensible contrasting behavior has been observed in the case of hydration of silicates with heavy water as far as the kinetics of new phase formation is concerned (see Fig. 1 for hydration of tricalcium silicate with a heavy water to cement ratio of 30%). The domain size of the density fluctuations grows in the beginning for a while, and subsequently appears to decrease with time, reaching saturation ultimately. In the case of hydration of silicates with heavy water, the microstructure of the hydrating mass undergoes a transition from mass fractal to surface fractal and subsequently to mass fractal. The scaling phenomenon, with all possible measures of the characteristic length, has not been established for the hydration of silicates with heavy water. It is a conjecture that the different rates of diffusion of light and heavy water in forming a gel structure in silicates lead to the formation of different structural networks with different scattering contrasts (Fig. 2).

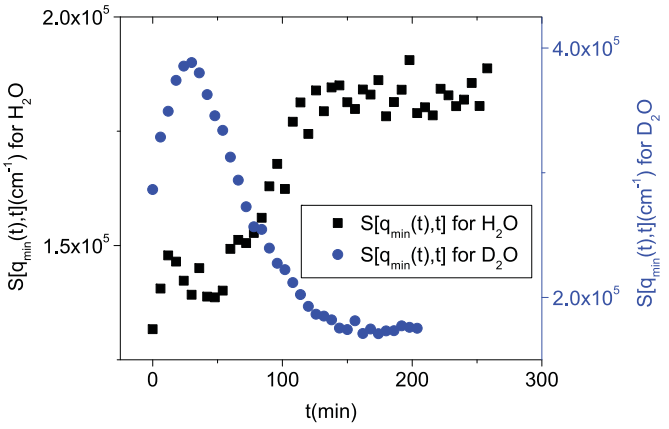

FIG. 2. (Color online) Temporal evolution of $S(q_{\min}(t),t)$ for light water and heavy water hydrating silicates (Ref. 1) where $S(q,t)$ represents the scattering function and $q_{\min}$ is the lowest attained q value for a particular measurement. It resembles the temporal evolution of η and $[L(t)]^2$ for light and heavy water hydration (Fig. 1). We have considered only a typical representative figure here.

In recent past, a Monte Carlo simulation, for embedded Euclidean dimension of 2, has been attempted to explain the aforementioned incomprehensible observations.[16] This simulation could explain only a few of the experimental results for light water hydrating a cement paste, by employing the concept of a deposition mechanism of the C-S-H gel in the available spaces inside the fractal cluster. However, the contrasting features of the structural evolution when hydrated with heavy water could not be explained on the same footing. Further, the earlier simulation was performed in the embedded Euclidean dimension of 2 due to limitations in computing resources.

In the present paper, we proposed a computer model that elucidates the contrasting experimental observations during hydration of cement by both light and heavy water. The present simulation, unlike the earlier one, has also been extended to three dimensions (3D). Further, a theoretical model has been proposed to explain the temporal evolutions of the fractal dimension for both light water and heavy water hydration cases.

II. COMPUTER MODEL

In the present section, a Monte Carlo–based computer model will be described to elucidate the hydration reaction

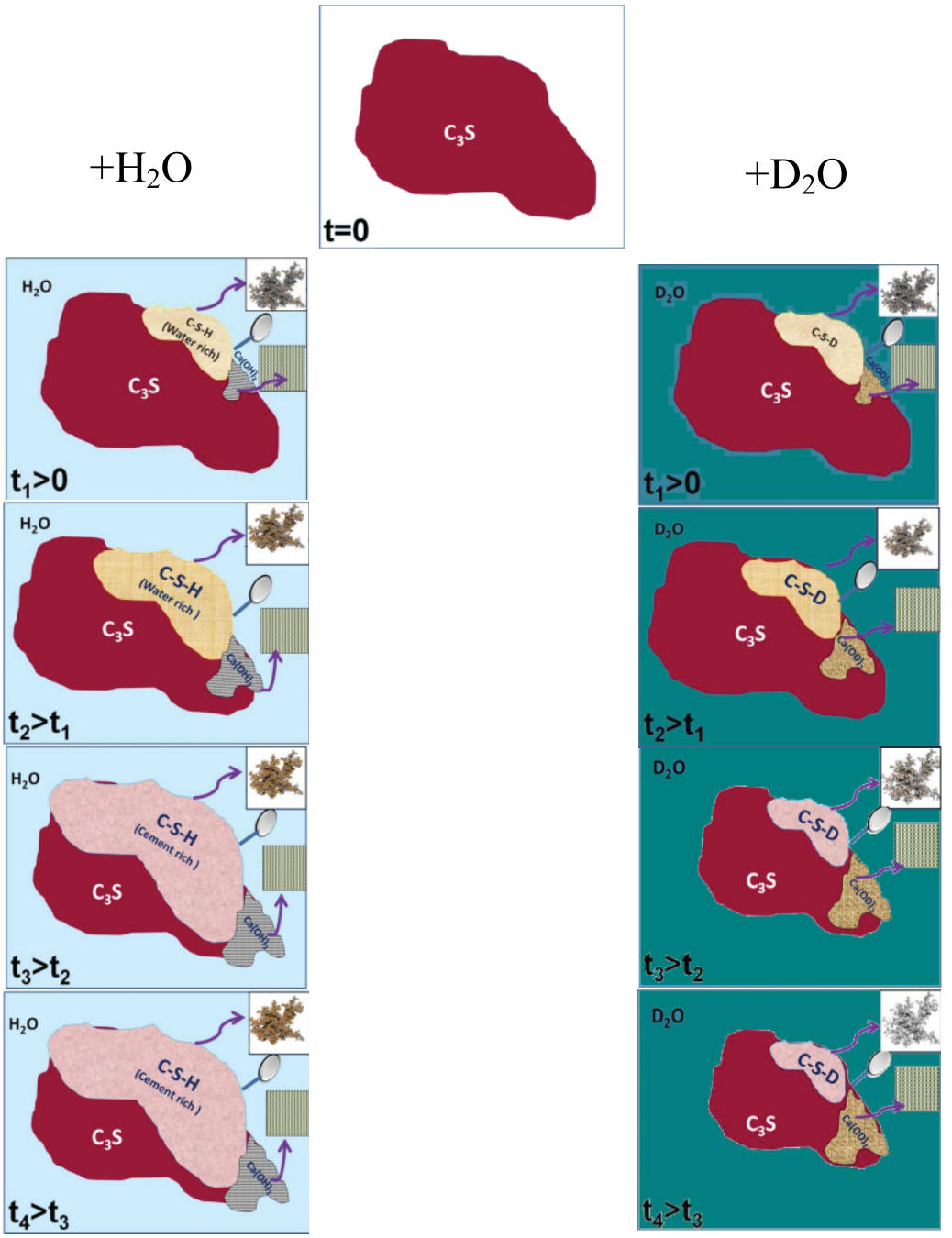

FIG. 3. (Color online) C_3S, main constituent of Portland cement (top) and temporal evolution of cement-water system during chemical reaction of C_3S with light water (on left) and with heavy water (on right). Microstructures of products of the reactions are indicated in the inset.

of cement particles with light water as well as heavy water. The temporal evolutions of the fractal dimension and the characteristic length of the system during hydration will be dealt with in both two and three dimensions.

Ordinary Portland cement is a composite material consisting of fine grains of tricalcium silicate $3CaO{\cdot}SiO_2$ (abbreviation C_3S; approximate mass percentage range 60%–80%) along with minor constituents like dicalcium silicate, tricalcium aluminate, tetracalcium iron aluminate, etc. Hydration of C_3S, the major component of Portland cement, by light water is described by the following chemical reaction:

$$3CaO.SiO_2 + (3 + y - x)H_2O \rightarrow (CaO)_x(SiO_2).(H_2O)_y + (3 - x)Ca(OH)_2 \quad (1)$$

where x is bounded by $0 \leqslant x \leqslant 3$ and y is bounded on one side, i.e., $y \geqslant 0$. $x = 3$ indicates hydration of C_3S without formation of $Ca(OH)_2$. That x is time dependent and the functional form of $x(t)$ is hydration medium (H_2O or D_2O) dependent have been

established[17] only recently. The *p*H dependence of the kinetics of the reaction is a plausible reason for the time dependence of $x(t)$. The product $(CaO)_x(SiO_2)\cdot(H_2O)_y$ (abbreviated as C-S-H, wherein hyphens indicate variable stoichiometry) is calcium silicate hydrate–a colloidal gel-like material.

In our model, we consider cement entirely made of C_3S, which is the major component of Portland cement, for simplicity. On mixing cement and light water, a complex series of hydration reactions[18] take place of which the main products are an amorphous calcium silicate hydrate (C-S-H) with gel-like structure and crystalline calcium hydroxide. The mesoscopic structure of the C-S-H gel determines the desirable properties of the hardened cement. The gel, having a non-Euclidean fractal morphology,[8,19–21] constitutes about 60–70 vol % of the fully hydrated cement paste, which is a composite wherein unreacted cement powder and $Ca(OH)_2$ crystals are embedded as shown in Fig. 3.

For a fractal system, a power-law relation exists between various physical parameters over a wide length scale. The volume $V(r)$ of such an object varies as r^{D_f} where D_f or the fractal dimension is less than 3 over a wide range of length scale. But for a Euclidean object in three dimensions, $D_f = 3$. Further, a fractal object that is generated following a particular mathematical rule is strictly self-similar and nonrandom in nature. However, for many natural and synthetic objects, the fractals are self-affine (i.e., have nonidentical scaling factors in different directions) and random in nature. A few of the computer models that have been proposed over the last two decades to simulate such random fractals originating from the agglomeration of smaller particles are diffusion-limited aggregation[22] (DLA), cluster-cluster aggregation,[23,24] tunable-dimension cluster-cluster aggregation,[25,26] reaction-limited cluster-cluster aggregation,[27] etc. It is worth mentioning that the fractal dimension obtained from the SANS experiment just at the onset of hydration (with both H_2O and D_2O) was found to be around 2.3. This prompted us to consider DLA as a possible initial cluster in order to understand the dynamical evolution of the fractal structure.

Diffusion-limited aggregation is a process of random aggregation, the isotropic standard form of which is constructed by a purely diffusive algorithm. No hydrodynamics is involved in forming such an aggregate. However, an aggregate may be formed by combining diffusion with hydrodynamics in an appropriate manner, such as viscous finger growth. It is worth mentioning here that there exist many evolution models with different growth rules which yield DLA at large scale but, at a smaller length scale, the structures could be different for different aggregation rules. However, many forms of diffusive growth with varying amounts of randomness exhibit DLA fractal morphology. Which growth rule is to be chosen is decided by the physical system that the aggregate is supposed to mimic. The structure of the aggregate depends on how the growth probability is distributed among different sites. What we need to determine are the growth probabilities of different sites for a given structure. This can be done for DLA and the way is to solve Laplace's equation for the potential when the cluster is considered to be made up of a conducting wire, kept at potential V. Then the electric field at different tips gives the growth probability at these tips. This then is similar to the solution of Laplace's equation in Darcy's law for viscous fingering aggregation. In Darcy flow, the governing equation is Darcy's law, which states that the Laplacian of pressure is constant. The constant depends on the rate of flow and can be made negligible. Then the governing aggregation equation is the same as that governing DLA. Alternatively, the mean density profile of a random DLA cluster may be related to the mean density profile of a viscous fingering pattern.

It is also assumed in DLA that the diffusing particles do not interact with one another in the sense that the motion of one particle is not affected by other particles. Each particle executes an independent random walk before sticking to the cluster growing around the seed or going outside the kill radius. If these diffusing particles move in a liquid, then the motion of one particle causes disturbances in the liquid which in turn affect the motion of other particles. If this process, known as the hydrodynamic effect of interaction, is important, then the motions of different particles cannot be thought of as being independent of one another—hydrodynamic interactions induce correlations in the motions of different particles.

But in the present problem, cement particles in contact with water molecules undergo hydration, and they do not have to diffuse through water over long distances. Hence, ignoring the hydrodynamic effect is justified. Further, the probability of sticking at different points in DLA is averaged over many evolutions with the same starting cluster, and the growth probability satisfies Laplace's equation with certain boundary conditions. The interaction of diffusing particles with one another or with molecules of the liquid medium is not required to determine the growth probability of a DLA cluster at different points along its perimeter as it is akin to the velocity of growth in a cluster of the same geometry in viscous fingering.

In the present work, simulation of a DLA cluster starts by keeping one particle at the origin of a lattice (later on this particle will be termed as seed) and allowing another particle, released from some release radius (r_0), to execute a random walk until it either touches the seed or goes out of some kill radius (r_k). A number of particles are thus released and some of them are finally aggregated around the seed to form a self-repetitive structure. For faster convergence of the simulation, some critical radius (r_c) is defined, beyond which particles take longer steps while after stepping into the radius they start taking shorter steps. r_o, r_k, and r_c can be adjusted intuitively to speed up the process. After obtaining a realizable DLA cluster in both 2D and 3D [Figs. 4(a) and 4(b)], the hydration reaction with light water was first simulated.

As soon as the hydration process starts, gel begins to be formed and as time passes this gel fills the available space in between the clusters to make a consolidated structure. However, it is understood that the growth of the cluster is constrained because of a similar response from adjacent clusters.

For the present calculation, it was considered that the DLA structure is surrounded by light water molecules. Although light water molecules were not represented explicitly, their reaction with C_3S was manifested in the following way. Firstly, one site was selected randomly from all the possible sites and then the cement particle occupying that site was replaced with product particles (for simplicity these will be called later gel particles) composed of gel and hydroxide. This is how one Monte Carlo (MC) step was completed. After repeating the same mechanism at various other sites, a layer of products was

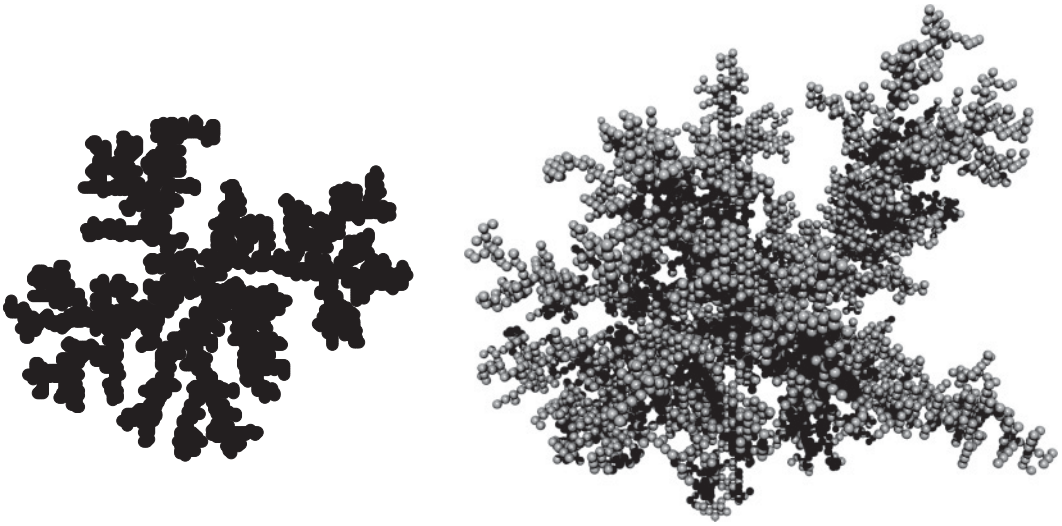

(a) (b)

FIG. 4. Initial DLA clusters in (a) two and (b) three dimensions.

formed on the cluster surface at the cost of cement particles. This layer restricts further reaction of water with cement and hence the probability of the hydration reaction is reduced. The fractal dimension (D_f) and characteristic length (L), giving a true flavor of the system characteristics, were evaluated at regular intervals of MC steps. Mathematically, the fractal dimension (D_f) is defined as

$$D_f = \frac{\log_{10}[N(\varepsilon)]}{\log_{10}\left(\frac{1}{\varepsilon}\right)}. \tag{2}$$

$N(\varepsilon)$ is the number of self-similar structures of linear size ε required to cover the entire fractal object. Numerically $N(\varepsilon)$ was calculated by the box counting method. The characteristic length was calculated from the radius of gyration (R_g) as defined below for the entire cluster with respect to an arbitrary origin:

$$R_g^2 = \frac{\int_V \rho(r) r^2 d^3 r}{\int_V \rho(r) d^3 r}. \tag{3}$$

It is to be noted that in earlier experiments[2] the radius of gyration was estimated from SANS data using the scattering length density (SLD) as the weighting function of the system. It can be shown that the SLD of tricalcium silicate ($\sim 3.94 \times 10^{14}\ \mathrm{m}^{-2}$) is greater than that of C-S-H gel ($\sim 2.29 \times 10^{14}\ \mathrm{m}^{-2}$) and less than that of C-S-D gel ($\sim 4.28 \times 10^{14}\ \mathrm{m}^{-2}$),[17] which are taken into consideration during the present simulation. In this model, the SLD of gel particles was scaled with respect to the SLD of cement particles.

In the case of hydration with heavy water, a similar kind of chemical reaction [i.e., Eq. (1)] as in the light water case is responsible, where C-S-D gel and $Ca(OD)_2$ are formed and it was incorporated into the simulation in an identical manner. But due to the stronger hydrogen bond—a chemical effect indeed—these newly formed C-S-D gel particles coalesce and a new kind of consolidated gel particle is formed. This was simulated by replacing a randomly picked cluster of product particles with a single particle, conserving the mass.

At the beginning of hydration, gel particles are less in number and therefore the probability that the gel particles coalesce into one is low. With time this probability goes up as the total number of gel particles formed in the hydration reaction increases. But after some time the probability comes down as very few gel particles will be left behind in the cluster to shrink.

The evolutions of D_f and $[L(t)]^2$ with MC steps for light and heavy water are shown in Figs. 5–7.

III. RESULTS AND DISCUSSION

Figure 4 depicts the initial DLA clusters, made by the random walk approach, in two as well as in three dimensions. As in the figure, the cluster is made of ~3200 cement particles for the 2D and ~5800 particles for the 3D case. The 2D cluster is introduced here just to show the morphological difference between 2D and 3D clusters. In the present study, hydration reactions with light and heavy water were simulated for the 3D cluster only as described in the previous section. The probability for a gel particle to be a part of an existing cluster is termed the sticking probability p. For the present simulation, various values, namely, 0.10, 0.25, 0.50, 0.75, and 1.00, of p have been considered. In the case of hydration with light water, gel particles try to fill the available space in and around the cluster. Therefore, an initial non-Euclidean morphology of the cluster tends toward a consolidated Euclidean morphology with progress in the hydration process. From Fig. 5(a), it is evident that the value of D_f of the cluster remains ~2.18 just at the onset of hydration. Thereafter, D_f increases with time, i.e., the cluster tends toward a Euclidean morphology. At around 5×10^4 MC steps, it reaches a plateau. This happens because the gel particles form a protective layer on the surface of the cluster and hence the hydration reaction stops unless and until there is a rupture of the protective layer. R_g^2 of the cluster also increases with time and finally reaches a plateau almost at the same time as D_f [Fig. 5(a)]. Since the SLD of C-S-H gel is less than that of C_3S, the cluster expands volumetrically as soon as the gel particles begin to form on the initial cluster. But the rate of expansion gradually gets reduced

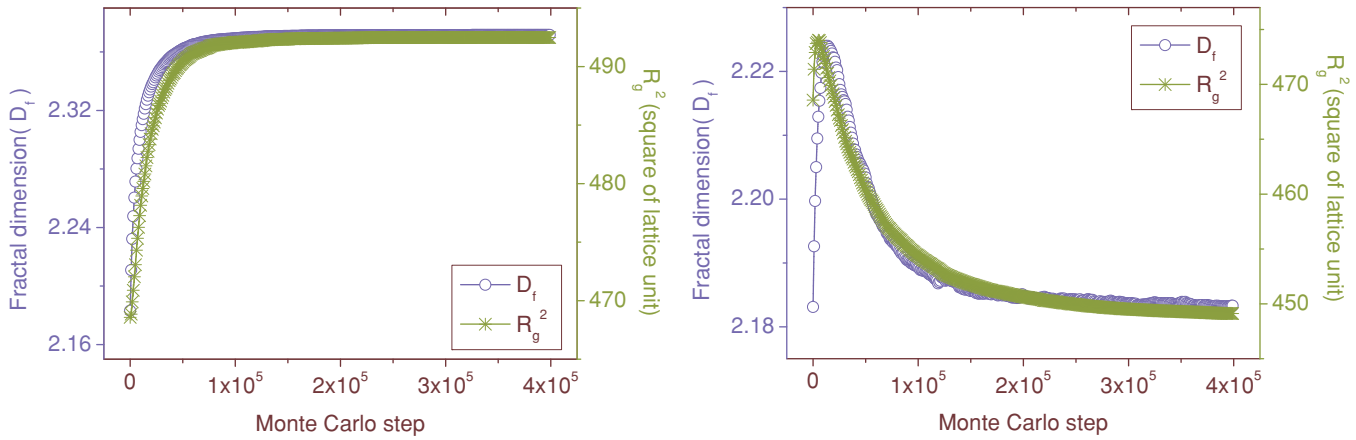

FIG. 5. (Color online) Variations of fractal dimension and square of characteristic length with number of Monte Carlo steps in (a) light water and (b) heavy water hydration cases. In both (a) and (b), the sticking probability was taken as unity.

due to the protective layer which hinders further gelation. Since the present computational work deals with a single cluster, it is difficult to realize the same percentage rise in R_g^2 as is observed experimentally. At the onset of hydration, neutrons, used as a probe in the experiment, are able to image all the isolated clusters. Due to incessant gelation, the clusters grow with time and gradually they are joined together to form a bigger cluster. As a consequence, the neutrons image only this bigger cluster; this is responsible for increase of R_g^2 with time in experiment.

In the case of hydration with heavy water, unlike the case of hydration with light water, the gel particles are formed first and then shrink due to the stronger hydrogen bond. Initially, the rate of shrinkage is dominated by the rate at which gel particles form. So at the onset of hydration, both R_g^2 and D_f increase and reach a peak, after which the shrinkage rate starts to surpass the formation rate and hence the curve turns down, i.e., the cluster again goes toward non-Euclidean morphology with increase of deviation from the corresponding Euclidean morphology. From Fig. 5(b), it is seen that D_f reaches its peak at about 1.4×10^4 MC steps and after that gradually decreases with time. A similar trend is observed for R_g^2 also [Fig. 5(b)]. Stronger hydrogen bonds involving deuterium atoms lead to consolidation of the gel at the later stages of hydration of cement with heavy water. This leads to R_g^2 decreasing with time. But its percentage rise and fall do not correlate exactly with experimental observation for the reason mentioned earlier.

One outcome of the present simulation is the effect of the sticking probability p on the time at which D_f or R_g^2 reaches the plateau (in the case of H_2O) or attains a maximum value (in the case of D_2O). A smaller sticking probability implies less affinity for sticking of the gel particles to the cement particles. Hence, the cluster evolves with a slower kinetics and the respective curves reach their plateau or peak at a later time. In Figs. 6(a) and 7(a), D_f and R_g^2, respectively, reach their plateaus for $p = 1.00, 0.75$, and 0.50, whereas the plateau is not reached for the cases with $p = 0.25$ and $p = 0.10$. In Figs. 6(b) and 7(b), the peaks are shifted toward higher numbers of MC steps with the decrease in p value.

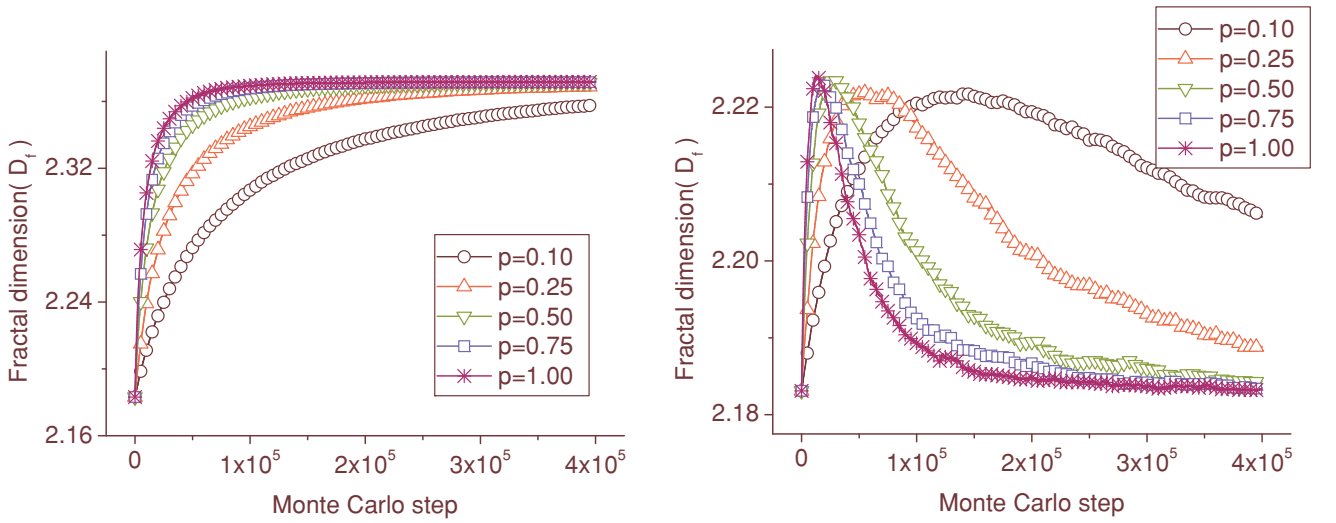

FIG. 6. (Color online) Variations of fractal dimension with number of Monte Carlo steps for different sticking probabilities in (a) light water and (b) heavy water hydration cases.

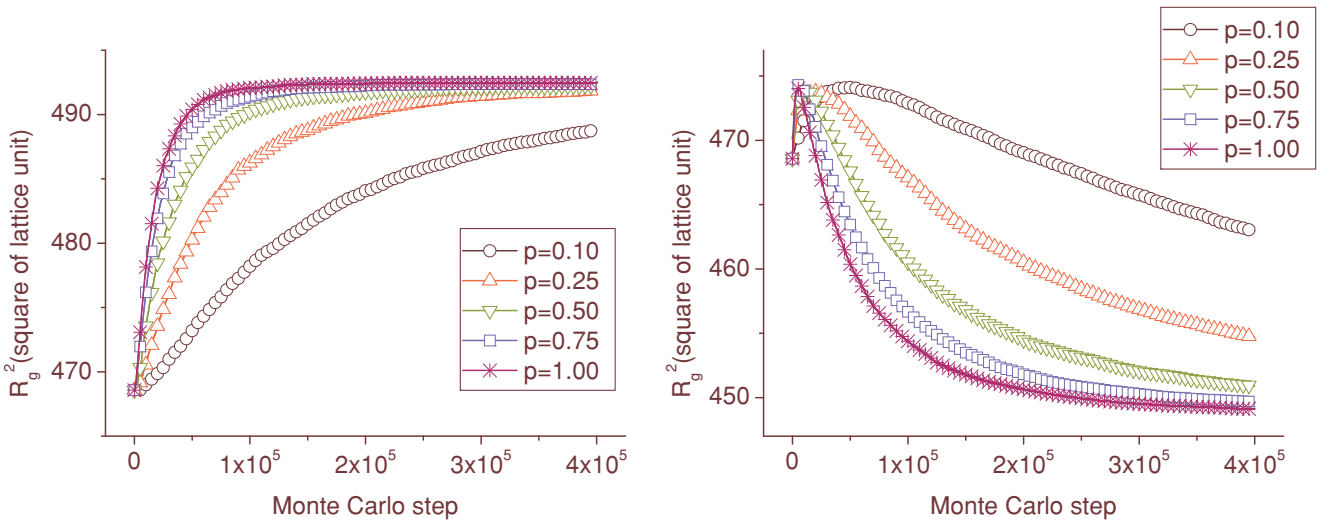

FIG. 7. (Color online) Variations of square of characteristic length with number of Monte Carlo steps for different sticking probabilities in (a) light water and (b) heavy water hydration.

As the theme of the present study was motivated by earlier results[1,2,9,16] for the small-angle scattering function, the evolution of the scattering function for the cluster has been studied here. The scattering function $S(q,t)$ is expressed as

$$S(q,t) = CP(q)Q(q,t), \tag{4}$$

where C is a scale factor and independent of q. For simplicity $P(q)$ was taken as a form factor of a sphere with radius $\tilde{r}_0$

$$P(q) = \frac{[\sin(q\tilde{r}_0) - q\tilde{r}_0\cos(q\tilde{r}_0)]^2}{(q\tilde{r}_0)^6} \tag{5}$$

and $Q(q,t)$ was taken as that for a mass fractal[12,28]

$$Q(q,t) = 1 + \frac{1}{(q\tilde{r}_0)^{D_f(t)}} \frac{D_f(t)\Gamma(D_f(t)-1)}{\left[1+\frac{1}{q^2\zeta^2}\right]^{\frac{(D_f(t)-1)}{2}}} \times \sin[(D_f(t)-1)\tan^{-1}(q\zeta)], \tag{6}$$

where ζ is the upper cutoff of the fractal and has been taken the same as the characteristic length scale. The evolutions of scattering functions for the H_2O and the D_2O cases are depicted in Figs. 8(a) and 8(b), respectively. The insets show the variation of the scattering intensity at $q \sim 0$. It is interesting to note from the figures that the scattering profiles evolve differently with time for the H_2O and D_2O cases. The evolutions resemble the trends as observed in the earlier scattering experiments.

Figure 9 shows the morphological difference between clusters when hydrated with light and heavy water. At 10^3 MC steps, there is no significant difference between them as both the clusters grow with time due to gel formation. But in subsequent MC steps, since the C-S-D gel starts to shrink whereas the C-S-H gel continues to be formed without any contraction of the matrix, the resultant clusters become different. It is evident from the figure that the light-water-hydrated cluster grows with time while the heavy-water-hydrated cluster, in

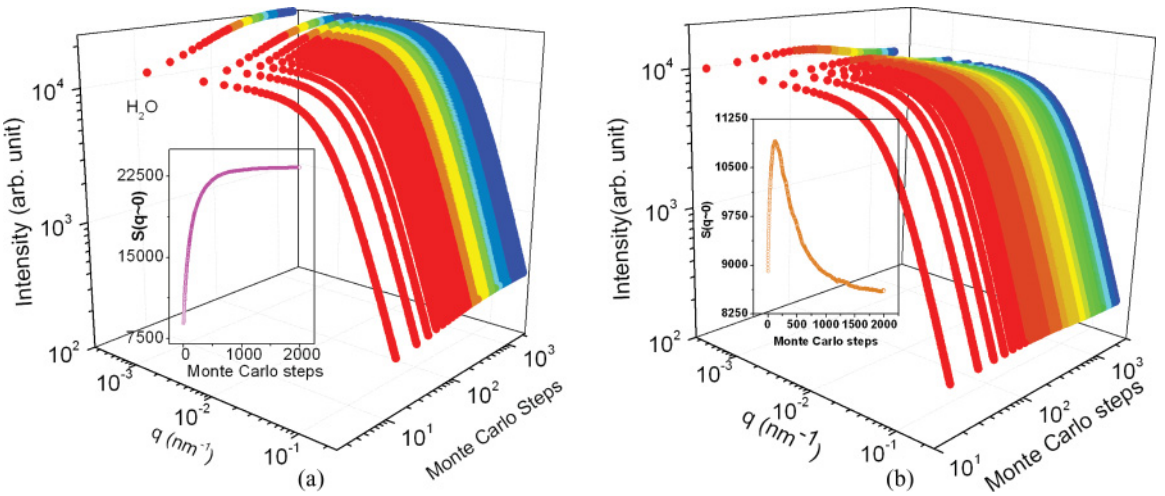

FIG. 8. (Color online) Evolutions of the simulated scattering profile with number of Monte Carlo steps at different q values for (a) light water and (b) heavy water hydration cases. Insets show the evolution of simulated scattering intensity with number of Monte Carlo steps at $q \sim 0$ for each case.

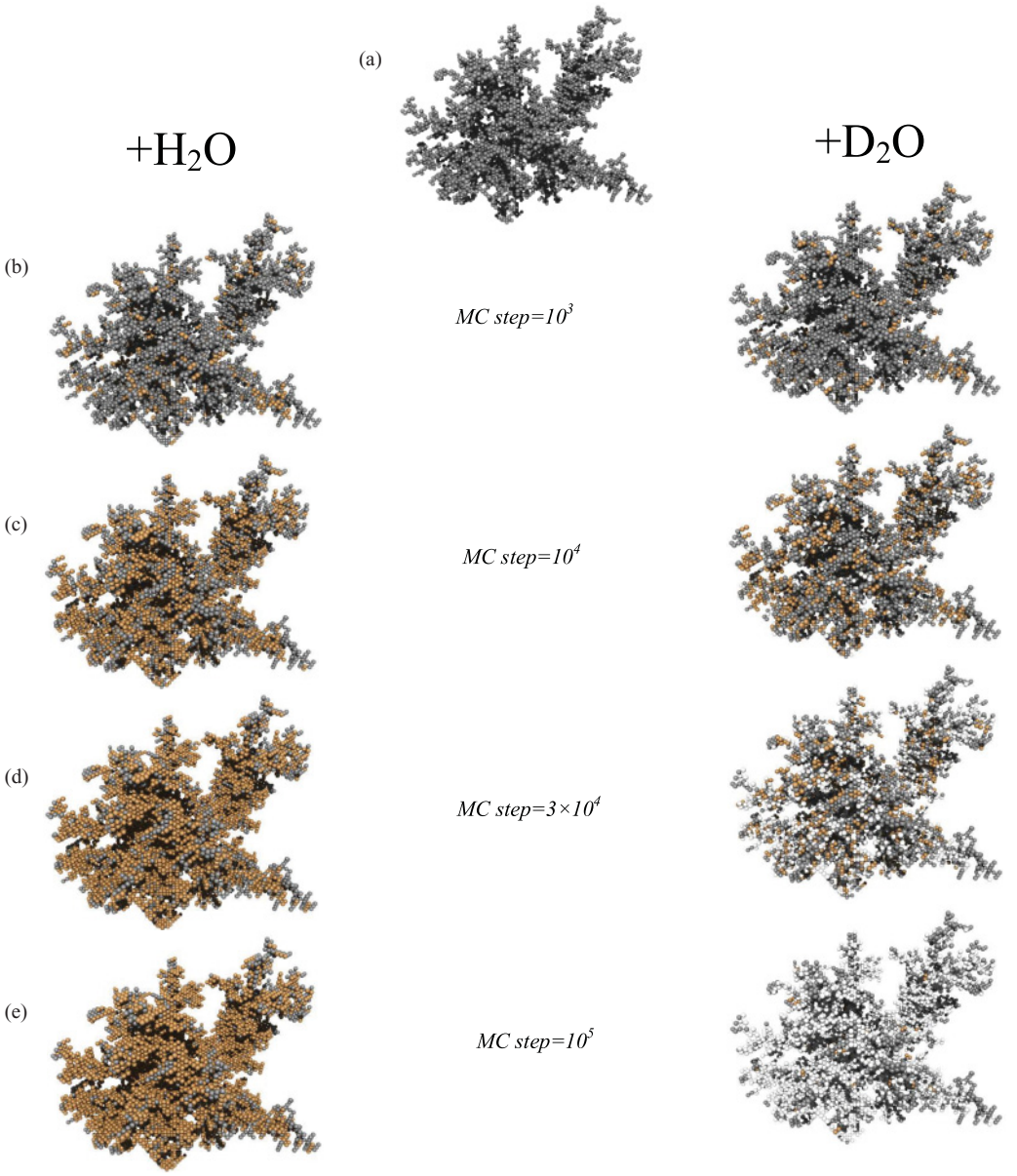

FIG. 9. (Color online) (a) Initial DLA cluster. (b)–(e) Evolution of DLA cluster when hydrated with light water (on left) and heavy water (on right) at different numbers of MC steps indicated in the figure.

spite of a little sign of growth at the onset of hydration, finally shrinks in size.

At this juncture, let us try to understand the simulation results on the basis of a proposed growth model associated with the rate equation. Let $N_{\rm ci}(t)$ be the number of cement particles situated inside the cluster, $N_{\rm cs}(t)$ the number of cement particles at the boundary surface of the cluster, and $N_g(t)$ the number of gel particles. Due to the presence of a protective layer at the boundary, $N_{\rm ci}(t)$ does not change with time and hence $N_{\rm ci}(t)$ is written as $N_{\rm ci}$.

For the present model calculation, we assume $3 + y - x = 1$ in the chemical reaction [i.e., Eq. (1)] of hydration of cement, a plausible case indeed. Therefore, the temporal variation of $N_{\rm cs}(t)$ is dictated by the following rate equation:

$$\frac{dN_{\rm cs}(t)}{dt} = -K_{c\to g} N_{\rm cs}(t) N_w(t), \tag{7}$$

where $K_{c\to g}$ is the rate constant of the above reaction and $N_w(t)$ represents the number of light water molecules. The assumption $3 + y - x = 1$ implies $N_w(t) - N_{\rm cs}(t) = c$, where c is a time-independent constant which depends on the initial concentrations of reactant molecules. Now, replacing $N_w(t)$ by $N_{\rm cs}(t) + c$ in Eq. (7) and solving the differential equation, we have

$$N_{\rm cs}(t) = \frac{c}{\left(1 + \frac{c}{N_{\rm cs}(0)}\right) e^{cK_{c\to g}t} - 1}. \tag{8}$$

The present simulation assumes that gel particles are formed with a higher rate compared to the depletion rate of cement particles in order to account for the volumetric expansion of the cluster. Since $N_g(0) = 0$,

$$N_g(t) = \tilde{\eta}\left(N_{\rm cs}(0) - N_{\rm cs}(t)\right), \tag{9}$$

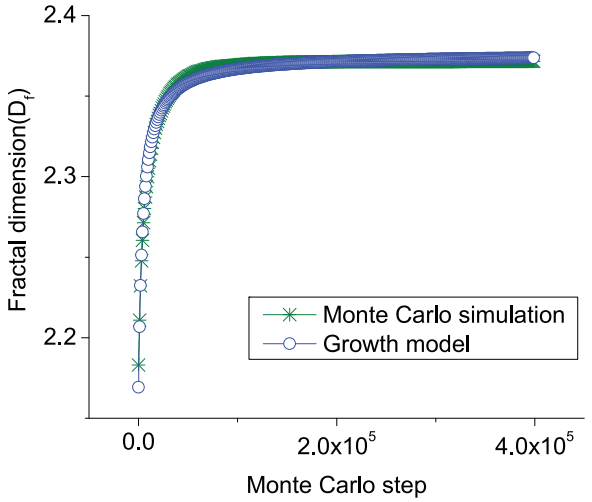

FIG. 10. (Color online) Fitting of D_f vs. number of MC steps for light water hydration of cement as in Fig. 4(a) with Eq. (10) in the proposed growth model for $L \sim 0.26$, $N_{ci} \sim 6.72 \times 10^2$, $\tilde{\eta} \sim 2.45$, $N_{cs}(0) \sim 3.83 \times 10^3$, $c \sim 1.00 \times 10^{-5}$, $K_{c\to g} \sim 3.81 \times 10^{-8}$ min.$^{-1}$. This is not a unique set of values. It varies depending on the guessed values provided before the fitting starts, which implies that the same temporal variation of D_f is possible for clusters of different morphology.

where $\tilde{\eta}$ is the ratio of formation rate of gel particles and depletion rate of cement particles.

The total number of cement and gel particles at time t becomes

$$N(t) = N_{ci} + \tilde{\eta} N_{cs}(0) + \frac{c(1-\tilde{\eta})}{\left(1 + \frac{c}{N_{cs}(0)}\right) e^{cK_{c\to g}t} - 1}. \quad (10)$$

Therefore, the fractal dimension (D_f) can be written as

$$D_f(t) = \frac{\log_{10}(N(t,\varepsilon))}{\log_{10}\left(\frac{1}{\varepsilon}\right)} = L \log_{10}\left(N_{ci} + \tilde{\eta} N_{cs}(0) + \frac{c(1-\tilde{\eta})}{\left(1 + \frac{c}{N_{cs}(0)}\right) e^{cK_{c\to g}t} - 1}\right), \quad (11)$$

where $L = [\log_{10}(1/\varepsilon)]^{-1}$.

Figure 5(a) can be fitted with Eq. (11) (Fig. 10). Hence, the above equation is proposed as a fitting function for the curve D_f vs MC steps in the case of light water.

It is evident from Fig. 10 that the variation of D_f with number of Monte Carlo steps obtained from simulation, and so the corresponding experimental observations also, correlates well with the temporal variation of D_f predicted by the growth model for the case of hydration of cement with light water. In this context, the relation between number of MC steps and real time of hydration is addressed in Fig. 11. Identical change in D_f is first identified in both experiment and simulation and then the corresponding changes in time and number of MC steps are worked out. This equivalence helps us to relate the computer model to the real hydration process and hence to confirm that the model is realistic.

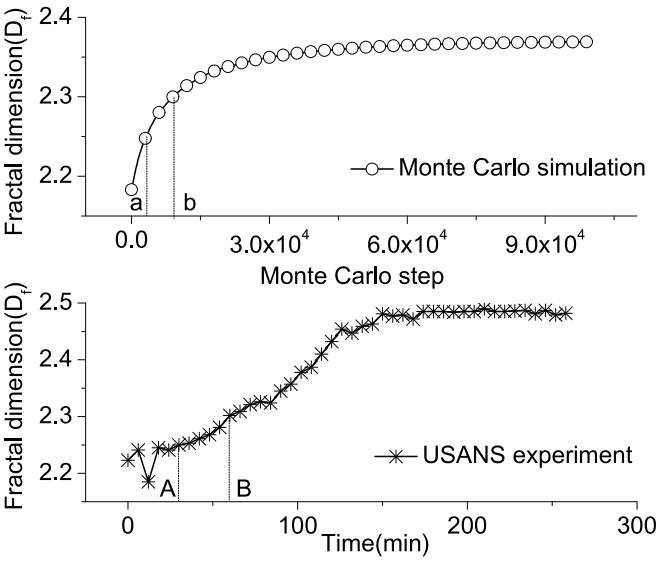

FIG. 11. Variation of D_f with number of MC steps and real time of hydration in the case of light water hydration. In the dotted sections, D_f changes from 2.25 to 2.3 for both cases and the corresponding change in number of MC steps is $(b-a) = 5800$ MC steps and in real time is $(B-A) = 30$ min. $(b-a)/(B-A) \sim 193$ MC steps/min i.e. the change that 193 MC steps bring about into the simulated system, occurs in 1 min. in the real system. But this factor varies depending on the state of the system in different time regimes.

In the case of hydration of cement by heavy water, C-S-D gel is not only formed but also shrinks. Let us assume that ξ number of gel particles coalesce to form a single consolidated gel particle. Hence, this two-step reaction can be simply written as $c \to \tilde{\eta} g$ in first step as in the earlier case of hydration and $\xi g \to G$ in second step, where, c, g and G represent cement, C-S-D gel, and consolidated gel, respectively. Therefore,

$$\frac{dN_g(t)}{dt} = -\tilde{\eta}\frac{dN_{cs}(t)}{dt} - K_{g\to G} N_g^{\xi}(t), \quad (12)$$

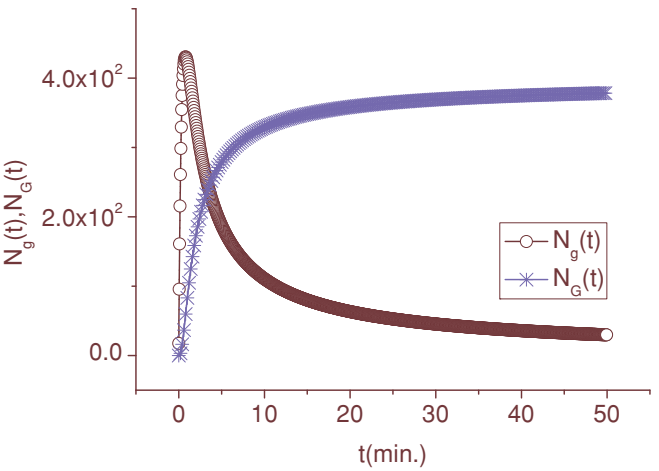

FIG. 12. (Color online) $N_g(t)$ vs. t and $N_G(t)$ vs. t as proposed in growth model with $\tilde{\eta} \sim 2.45$, $N_{cs}(0) \sim 3.83 \times 10^3$, $c \sim 1.00 \times 10^{-5}$, $K_{c\to g} \sim 4.85 \times 10^{-3}$ min.$^{-1}$, $K_{g\to G} \sim 3.35 \times 10^{-4}$ min.$^{-1}$, $\xi \sim 2.25$. This is not a unique set of values for the reason already mentioned in Fig. 10.

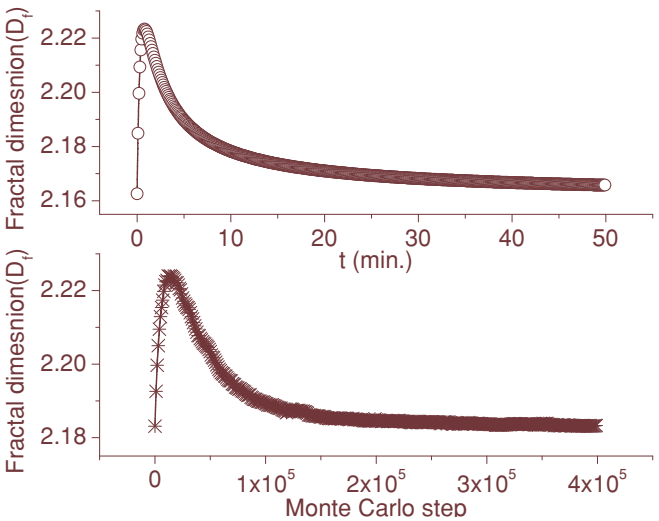

FIG. 13. D_f vs. t as proposed in growth model with $L \sim 0.31$, $N_{ci} \sim 7.20 \times 10^2$, $\tilde{\eta} \sim 2.45$, $N_{cs}(0) \sim 3.83 \times 10^3$, $c \sim 1.00 \times 10^{-5}$, $K_{c\to g} \sim 4.85 \times 10^{-3}$ min.$^{-1}$, $K_{g\to G} \sim 3.35 \times 10^{-4}$ min^{-1}, $\xi \sim 2.25$ (top). D_f vs. number of MC steps for heavy water hydration of cement by computer model (bottom). This is not a unique set of values for the reason already mentioned in Fig. 10.

where $K_{g\to G}$ is the rate constant for the second step of the reaction.

Now, the formation rate of the consolidated gel particles is given by

$$\frac{dN_G(t)}{dt} = \frac{1}{\xi} K_{g\to G} N_g^{\xi}(t), \tag{13}$$

where $N_G(t)$ is the number of new gel particles and $1/\xi$ is the ratio of the formation rate of new gel particles and the depletion rate of the precursor. The temporal variation of $N_g(t)$ and $N_G(t)$ are shown in Fig. 12.

In this case, the fractal dimension (D_f) is expressed as

$$D_f(t) = \frac{\log_{10}[N(t,\varepsilon)]}{\log_{10}\left(\frac{1}{\varepsilon}\right)} = L\log_{10}\left(N_{ci} + \frac{c}{\left(1+\frac{c}{N_{cs}(0)}\right)e^{cK_{c\to g}t}-1} + N_g(t) + N_G(t)\right) \tag{14}$$

where $L = [\log_{10}(1/\varepsilon)]^{-1}$. Equation (14) reproduces the same kind of variation of D_f with time (in experiment) as well as with MC steps (in simulation) observed in heavy water hydration of cement (Fig. 13).

It is evident from Fig. 13 that the variation of D_f with number of Monte Carlo steps obtained from simulation, and so the corresponding experimental observations also, correlates well with the temporal variation of D_f predicted by the growth model for the case of hydration of cement with heavy water.

IV. CONCLUSIONS

In accordance with the present Monte Carlo–based computer model, the space filling mechanism of C-S-H gel is the key to analyzing the temporal variation of the fractal dimension and characteristic length in the case of light water hydration whereas for the hydration with heavy water, both filling and shrinkage of the C-S-D gel are responsible for the contrasting temporal behavior of the above-mentioned physical quantities. The radius of gyration, which involves the scattering length density of the gel, was considered to be the characteristic length in the simulation. A growth model was proposed to explain only the temporal behavior of the fractal dimension for both light and heavy water hydration cases and its results agree well with the experimental observations and Monte Carlo simulation results. The equations coming out of the model [i.e., Eqs. (11) and (14)] may look complicated, but suitable mathematical adjustments (like merging two or three parameters into one etc.) can make them simpler. But any such mathematical simplification was not done since the focus was on finding the best-fit values of each and every parameter involved in the equations so that, if any measurement of those parameters is done in future, the measurement results can be linked with these best-fit values. Hence, the present calculations demand further experiments in future. Moreover, an extension of the present theoretical model for the evolution of the radius of gyration during light and heavy water hydration of cement will be considered in the near future. It is important to mention that the entire analysis is applicable for hydration observed on a short time scale. Its long-time behavior still remains unknown and hence it demands more detailed scattering investigations.

ACKNOWLEDGMENT

We acknowledge the discussion one of us (S.M.) had with D. Dhar in regard to the computer modeling.

*smazu@barc.gov.in

[1] S. Mazumder, D. Sen, A. K. Patra, S. A. Khadilkar, R. M. Cursetji, R. Loidl, M. Baron, and H. Rauch, Phys. Rev. Lett. **93**, 255704 (2004).

[2] S. Mazumder, D. Sen, A. K. Patra, S. A. Khadilkar, R. M. Cursetji, R. Loidl, M. Baron, and H. Rauch, Phys. Rev. B **72**, 224208 (2005).

[3] R. D. Lorentz, A. Bienenstock, and T. I. Morrison, Phys. Rev. B **49**, 3172 (1994).

[4] M. J. Regan and A. Bienenstock, Phys. Rev. B **51**, 12170 (1995).

[5] S. Mazumder, D. Sen, I. S. Batra, R. Tewari, G. K. Dey, S. Banerjee, A. Sequeira, H. Amenitsch, and S. Bernstorff, Phys. Rev. B **60**, 822 (1999).

[6] R. Tewari, S. Mazumder, I. S. Batra, G. K. Dey, and S. Banerjee, Acta Materialia, **48**, 1187 (2000).

[7] D. Sen, S. Mazumder, R. Tewari, P. K. De, H. Amenitsch, and S. Bernstorff, J. Alloys Compd. **308**, 250 (2000).

[8] M. Kriechbaum, G. Degovics, J. Tritthart, and P. Laggner, Prog. Colloid Polym. Sci. **79**, 101 (1989).

[9] S. Mazumder, R. Loidl, and H. Rauch, Phys. Rev. B **76**, 064205 (2007).

[10]M. Hennion, D. Ronzaud, and P. Guyot, Acta Metall. **30**, 599 (1982).
[11]S. Katano and M. Iizumi, Phys. Rev. Lett. **52**, 835 (1984).
[12]T. Freltoft, J. K. Jems, and S.K. Sinha, Phys. Rev. B **33**, 269 (1986).
[13]D. F. R. Mildner and P. L. Hall, J. Phys. D **19**, 1535 (1986).
[14]S. Komura, K. Osamura, H. Fujii, and T. Takeda, Phys. Rev. B **30**, 2944 (1984).
[15]J. J. Katz, Am. Scientist **48**, 544 (1960).
[16]D. Sen, S. Mazumder, and J. Bahadur, Phys. Rev. B **79**, 134207 (2009).
[17]S. Mazumder, D. Sen, J. Bahadur, J. Klepp, H. Rauch, and José Teixeira, Phys. Rev. B **82**, 064203 (2010).
[18]B. Rodmacq, M. Maret, J. Laugier, L. Billard, and A. Chamberod, Phys. Rev. B **38**, 1105 (1988).
[19]A. Heinemann, H. Hermann, K. Wetzig, F. Haeussler, H. Baumbach, and M. Kroening, J. Mater. Sci. Lett. **18**, 1413 (1999).
[20]R. A. Livingston, D. A. Neumann, A. J. Allen, S. A. Fitzgerald, and R. Berliner, Neutron News **11**, 18 (2000).
[21]Douglas Winslow, John M. Bukowski, and J. Francis Young, Cem. Concr. Res. **25**, 147 (1995).
[22]T. A. Witten Jr. and L. M. Sander, Phys. Rev. Lett. **47**, 1400 (1981).
[23]P. Meakin, Phys. Rev. Lett. **51**, 1119 (1983).
[24]M. Koib, R. Botet, and R. Jullien, Phys. Rev. Lett. **51**, 1123 (1983).
[25]R. Thouy and R. Jullien, J. Phys. A **27**, 2953 (1994).
[26]R. Thouy, R. Jullien, J. Phys. I France **6**, 1365 (1996).
[27]Paul Meakin and Fereydoon Family, Phys. Rev. A **38**, 2110 (1988).
[28]J. Texeira, J. Appl. Cryst. **21**, 781 (1988).